blood®
Regular Article

LYMPHOID NEOPLASIA

Somatic IL4R mutations in primary mediastinal large B-cell lymphoma lead to constitutive JAK-STAT signaling activation

Elena Viganò,[1,2,*] Jay Gunawardana,[1,2,*] Anja Mottok,[1-4] Tessa Van Tol,[1] Katina Mak,[1] Fong Chun Chan,[1,2] Lauren Chong,[1] Elizabeth Chavez,[1] Bruce Woolcock,[1] Katsuyoshi Takata,[1] David Twa,[1,2] Hennady P. Shulha,[1] Adèle Telenius,[1] Olga Kutovaya,[1,2] Stacy S. Hung,[1] Shannon Healy,[1,2] Susana Ben-Neriah,[1] Karen Leroy,[5] Philippe Gaulard,[6-8] Arjan Diepstra,[9] Robert Kridel,[1,2] Kerry J. Savage,[1] Lisa Rimsza,[10] Randy Gascoyne,[1,2] and Christian Steidl[1,2]

[1]Department of Lymphoid Cancer Research, British Columbia Cancer Agency, Vancouver, Canada; [2]Department of Pathology and Laboratory Medicine, University of British Columbia, Vancouver, Canada; [3]Institute of Pathology, University of Würzburg, Würzburg, Germany; [4]Comprehensive Cancer Centre Mainfranken, Würzburg, Germany; [5]University Paris Descartes, Paris, France; [6]Département de Pathologie–Service d'Hématologie–Plateforme de Ressources Biologiques, Groupe Hospitalier Henri-Mondor, Assistance Publique–Hôpitaux de Paris, Créteil, France; [7]INSERM U955, Créteil, France; [8]Université Paris Est, Créteil, France; [9]Department of Pathology and Medical Biology, University of Groningen, University Medical Center Groningen, Groningen, The Netherlands; and [10]Department of Pathology, University of Arizona, Tucson, AZ

KEY POINTS

- **Somatic *IL4R* mutations were identified in 24% of primary PMBCL cases (n = 62) and in 100% of PMBCL-derived cell lines.**
- **IL4R mutations lead to hyperphosphorylation of STAT proteins activating downstream immunoregulatory genes (CD23, CCL17).**

Primary mediastinal large B-cell lymphoma (PMBCL) is a distinct subtype of diffuse large B-cell lymphoma thought to arise from thymic medullary B cells. Gene mutations underlying the molecular pathogenesis of the disease are incompletely characterized. Here, we describe novel somatic *IL4R* mutations in 15 of 62 primary cases of PMBCL (24.2%) and in all PMBCL-derived cell lines tested. The majority of mutations (11/21; 52%) were hotspot single nucleotide variants in exon 8, leading to an I242N amino acid change in the transmembrane domain. Functional analyses establish this mutation as gain of function leading to constitutive activation of the JAK-STAT pathway and upregulation of downstream cytokine expression profiles and B cell–specific antigens. Moreover, expression of I242N mutant IL4R in a mouse xenotransplantation model conferred growth advantage in vivo. The pattern of concurrent mutations within the JAK-STAT signaling pathway suggests additive/synergistic effects of these gene mutations contributing to lymphomagenesis. Our data establish *IL4R* mutations as novel driver alterations and provide a strong preclinical rationale for therapeutic targeting of JAK-STAT signaling in PMBCL. (*Blood*. 2018;131(18):2036-2046)

Introduction

Primary mediastinal large B-cell lymphoma (PMBCL) accounts for ~2% to 4% of all non-Hodgkin lymphomas (NHLs) affecting predominantly young female patients in their third and fourth decades of life. PMBCL is thought to arise from thymic medullary B cells and is clinically characterized by a large anterior mediastinal mass with a locally invasive growth pattern.[1] Historically, PMBCL was considered a subtype of diffuse large B-cell lymphoma (DLBCL), but subsequent molecular characterization highlighted a similar gene expression profile with the nodular sclerosis subtype of classical Hodgkin lymphoma (HL).[2-4] Because of its clinical, pathological, and genetic features, PMBCL was recognized as a distinct entity by the World Health Organization classification of lymphoid neoplasms in 2008.[5]

Recurrent somatic mutations in nuclear factor-κB (NF-κB) and JAK-STAT[6] signaling pathways, leading to their aberrant activation, constitute a hallmark of the disease.[7] The transcription factor NF-κB regulates proliferation, survival, development, and activation of immune cells,[8] and its deregulation provides survival and proliferative advantage to malignant cells. Indeed, chromosomal amplification of *REL* (2p16.1),[9] *BCL10* (1p22), and *MALT1* (18p21) gene loci,[10] as well as inactivating biallelic mutations of the negative NF-κB regulator *TNFAIP3*[11] have been characterized as leading to constitutively active nuclear NF-κB during PMBCL pathogenesis. Similar to NF-κB, genomic hits targeting the JAK-STAT pathway have been described, mostly in the setting of targeted single-gene mutational studies. Most prominently, genomic amplification of *JAK2* (9p24.1)[12] and somatic mutations affecting negative regulators, such as *SOCS1*[13] and the protein phosphatase *PTPN1*,[14] potentiate the activation of this oncogenic pathway.

More recently, the tumor microenvironment and its involvement in lymphomagenesis has been highlighted based on key

discoveries that linked somatic gene mutations with immune escape phenotypes[12,15,16] and emergence of breakthrough immunotherapies targeting microenvironment biology, such as immune checkpoint inhibition.[17-20] However, knowledge about somatic gene mutations underlying crosstalk of lymphoma cells with immune infiltrates and changes in microenvironment composition is very sparse. Proof of concept that microenvironment biology and immune privilege are important aspects of PMBCL pathogenesis was demonstrated in a previous study that established frequent alterations of *CIITA*, the master transcriptional regulator of major histocompatibility complex (MHC) class II expression, to underlie loss of MHC class II expression in a subgroup of patients, a finding that correlated with a reduced number of cytotoxic T cells and T helper cells in the tumor microenvironment.[21] Moreover, structural genomic changes of chromosome 9p24.1 have been shown to lead to increased expression of the programmed death ligands PDL1 and PDL2 contributing to T-cell exhaustion.[12,16,22] However, very little is known about the role of somatic mutations affecting microenvironment biology and its contribution to pathogenesis.

In this study, we characterize novel somatic alterations occurring in the interleukin 4 receptor (IL4R) in PMBCL. Specifically, we uncover a recurrent hotspot mutation in the IL4R transmembrane domain (NP_000409.1, p.I242N) that leads to constitutive JAK-STAT activation, growth advantage in vivo, and an altered cytokine expression profile. Moreover, we show the presence of multiple mutational hits in the JAK-STAT pathway (*JAK2*, *SOCS1*, *STAT6*, *PTPN1*, and *IL4R*) in primary specimens, suggesting a synergistic/additive effect of these mutations in PMBCL pathogenesis.

Methods

Tissue specimens, cell lines

Specimens from 62 PMBCL patients were selected from the tissue archives of the Centre for Lymphoid Cancer of the British Columbia Cancer Agency, the Arizona Lymphoma Repository, and the Hôpital Henri Mondor Pathology Department according to the availability of fresh-frozen lymphoid tissue biopsy material and clinical follow-up data. Additional information is reported in supplemental Methods (available on the *Blood* Web site).

Screening for *IL4R* somatic mutations

IL4R mutations were detected by deep amplicon sequencing and were subsequently validated by Sanger sequencing.

IL4R expression, site-directed mutagenesis, reporter gene assay in HEK293-STAT6 cells

The wild-type (WT) *IL4R* coding sequence was amplified by polymerase chain reaction (PCR) using complementary DNA from Karpas 1106P and cloned into the pcDNA3.1 mammalian expression vector (Invitrogen). The *IL4R* I242N mutation was created using the QuikChange XL site-directed mutagenesis kit (Agilent Technologies) according to the manufacturer's instructions. The remaining *IL4R* mutations (D37N, Y62C, N78Y, G113D, F115L, N176S, R200W, C251W, K308N, E684Kfs*2) were created using the GENEART site-directed mutagenesis system (Thermo Fisher Scientific) according to the manufacturer's instructions. Empty pcDNA3.1 was used as a mock-vector. The plasmids were purified by Spin Miniprep kit (Qiagen) and 1 μg of plasmid was transfected into HEK293 cells expressing STAT6 (HEK293-STAT6; Invitrogen), seeded the day before at 0.25×10^6 cells/well (12 multiwell plate), using Lipofectamine2000 (Invitrogen). Twenty-four hours after transfection, cells were cultured in the absence or presence of recombinant human IL-4 (0.1 ng/mL, 24 hours) (R&D Systems) and secreted embryonic alkaline phosphatase (SEAP) levels assayed in cell-free supernatant according to the manufacturer's protocol.

Flow cytometry

Flow cytometry analysis for surface expression of IL4R (CD124) and CD23 was performed using an LSR Fortessa special order system (Becton-Dickinson Biosciences) as previously described.[15]

Quantitative RT-PCR

Total RNA was isolated using the RNeasy kit (Qiagen) and treated with DNAse I (Promega). TaqMan gene expression assay probes were used to detect messenger RNA (mRNA) levels.

Preparation of doxycycline-inducible cell lines, retroviral transduction, cell culture

Retroviral transduction of DEV cells was performed as previously described.[23,24]

Western blotting, immunoprecipitation

Western blotting and immunoprecipitation were performed as previously described in Gunawardana et al[14] and Rui et al.[25]

Whole-transcriptome sequencing

RNA sequencing (RNA-Seq) was performed as previously described using RNA extracted from DEV cells expressing IL4R WT and I242N.[26]

Gene expression by complementary DASL assay

The Illumina Whole-Genome DNA-mediated annealing, selection, extension, ligation (DASL) assay was performed on 400 ng of RNA derived from 42 PMBCL tissue specimens (32 cases were *IL4R* WT and 10 had mutations in the *IL4R* gene) by The Centre for Applied Genomics (The Hospital for Sick Children, Toronto, Canada), as previously published.[27]

Murine xenograft model

The animal study was performed according to the animal care protocol approved by the Institutional Animal Care Committee (University of British Columbia). DEV cells in growth medium (2×10^6) were mixed with Matrigel matrix (1:1 ratio, 100 μL) and implanted subcutaneously into the back of female NSG mice using a 27-gauge needle. Tumor growth was monitored by measuring tumor dimensions with calipers beginning on observance of palpable tumors. Tumors were allowed to grow to a maximum of 800 mm^3 before animals were euthanized (the first mouse tumor was culled on day 24 and the last mouse tumor on day 51). Following necropsy, part of the tumor was snap-frozen for further molecular studies and part of the tumor was fixed in 10% neutral buffered formalin and processed for histopathological evaluation (hematoxylin and eosin [H&E]) and Ki67 staining.

Immunohistochemistry

Immunohistochemistry (IHC) was performed on 4-μm whole tissue or tissue microarray sections on a Ventana Benchmark XT and details are described in supplemental Methods.

Statistical analysis

Comparisons between groups were performed using a 2-sample Student *t* test, 1-sample Student *t* test, 1-way analysis of variance (ANOVA) or 2-way ANOVA, where appropriate (GraphPad Prism 7). Time-to-event analyses were performed using the Kaplan-Meier method; survival curves were compared by the log-rank test using SPSS, version 14.0.

Results

IL4R is frequently mutated in PMBCL

We have previously described *IL4R* being mutated in 1 of 7 primary PMBCL specimens and 3 of 3 PMBCL cell lines analyzed by whole transcriptome sequencing.[14] To uncover the prevalence and type of genomic mutations affecting *IL4R*, we screened the complete coding sequence of *IL4R*, comprising 9 exons, in 62 primary PMBCL specimens by Sanger sequencing and deep amplicon sequencing. In total, after the exclusion of reported single nucleotide polymorphisms and synonymous mutations, we found 21 variants (16 mutations in 15 of 62 primary cases [24.2%] and 5 mutations in 3 of 3 cell lines [100%]) (supplemental Table 4), with 1 primary case and 2 cell lines harboring 2 mutations each. The majority of mutations (95.2%) were missense mutations; the exception was 1 frameshift mutation (4.8%) that putatively leads to premature IL4R protein termination from the introduction of a stop codon at amino acid position 686. The type, distribution, and frequency of mutations for each exon are shown in Figure 1A. Nine of the 16 mutations detected in primary cases (56.3%) showed a strikingly recurrent hotspot mutation in exon 8 (hg19: chromosome 16: 27,367,183; ENST00000395762.6, c.725T>A), which leads to the substitution of the isoleucine residue at amino acid position 242 by an asparagine (I242N). This recurrent mutation was confirmed as somatic by sequencing constitutional DNA extracted from peripheral blood in 1 patient (supplemental Figure 1).

IL4R mutations lead to STAT6 phosphorylation in engineered HEK 293 cells

To study the functional relevance of the *IL4R* I242N mutation, we ectopically expressed *IL4R* in engineered HEK293 cells expressing STAT6 (HEK293-STAT6). The expression of IL4R protein was increased in cells transfected with *IL4R* WT or mutants compared with cells transfected with empty vector alone (Figure 1B; supplemental Figure 2A-C). As expected, treatment of HEK293-STAT6 cells with recombinant IL-4 induced phosphorylation of STAT6 (supplemental Figure 2B,D) and STAT6-dependent expression of SEAP (Figure 1C; supplemental Figure 2E), but no significant difference was observed between cells transfected with WT, IL4R mutants, or empty vector. To determine if IL4R mutants affected the phosphorylation status of STAT6 in a ligand-independent manner, we analyzed cell lysates obtained from unstimulated cells by western blot. Interestingly, only HEK cells expressing the I242N, D37N, Y62C, N176S, and R200W mutated form of IL4R showed increased IL-4 independent phosphorylation of STAT6 (Figure 1B; supplemental Figure 2F), indicating constitutive activation of the JAK-STAT pathway. Consistently, a higher amount of SEAP was detected in supernatants from cells expressing these mutants compared with WT IL4R (Figure 1C), confirming the results obtained by western blot.

The activation of IL4R is known to induce additional downstream signaling pathways such as phosphoinositol 3-kinase-AKT and mitogen-activated protein kinase.[28] To evaluate the role of IL4R mutants in phosphoinositol 3-kinase-AKT and mitogen-activated protein kinase signaling pathways, we determined the phosphorylation of AKT and ERK1/2 in transfected HEK293-STAT6, respectively. Notably, only HEK293-STAT6 expressing the hotspot mutation (I242N) induced phosphorylation of ERK1/2, whereas no significant AKT activation was observed for any mutant (supplemental Figure 3A-B).

IL4R I242N mutation hyperphosphorylates STAT proteins activating downstream JAK-STAT signaling in lymphoma cells

To evaluate activation of the JAK-STAT pathway by *IL4R* I242N hotspot mutations in a B-cell lymphoma context, we expressed IL4R I242N (DEV IL4R^{I242N}) or IL4R WT (DEV IL4R^{WT}) in the nodular lymphocyte predominant HL-derived cell line DEV. Equally increased transcript expression of IL4R in DEV IL4R^{WT} and DEV IL4R^{I242N} was confirmed by quantitative reverse transcription PCR as compared with cells transduced with empty vector (Figure 2A). However, DEV IL4R^{I242N} cells showed lower IL4R protein levels (Figure 2B; supplemental Figure 4) and lower surface expression (Figure 2C-D) compared with DEV IL4R^{WT} cells. Following IL-4 stimulation, phosphorylation of STAT5 and STAT6 was increased in DEV empty, IL4R^{WT}, and IL4R^{I242N} cells (Figure 2B; supplemental Figure 4). In accordance with the lower expression of IL4R mutant on the surface (Figure 2C-D), mutant cells showed a less pronounced phosphorylation of STAT5 compared with WT cells upon stimulation with IL-4 (Figure 2B). Strikingly, the I242N mutant hyperphosphorylated STAT5 and STAT6 independent of IL-4 stimulation despite the lower levels in IL4R expression observed (Figure 2B; supplemental Figure 4). No appreciable changes in phospho-STAT3 levels were detected between WT and the mutant in both IL-4–stimulated and IL-4–unstimulated cells (Figure 2B). In addition, concordantly with the results obtained in HEK293-STAT6, DEV IL4R^{I242N} showed a slight increase in phospho-ERK1/2 compared with DEV IL4R^{WT}, but no difference in phospho-AKT was observed (supplemental Figure 5A-B).

The I242N mutation resides in the transmembrane domain of the protein and affects an evolutionarily conserved residue. The mutated residue is larger and more hydrophilic than the WT residue. Therefore, we investigated the subcellular localization of the mutant protein using fractionated western blot and found that IL4R remained in the membranous compartment of both WT and mutant cells (supplemental Figure 6A). Because membrane-bound IL4R can be proteolytically cleaved to form a soluble fraction, which has been reported to enhance IL-4 signaling,[29,30] we assayed secreted IL4R levels in WT and mutant cell culture supernatants by enzyme-linked immunosorbent assay (ELISA), but no significant differences were found (supplemental Figure 6B).

Mutant *IL4R* induces CD23 expression and CCL17 secretion

To determine genome-wide gene expression changes in DEV IL4R^{I242N} vs DEV IL4R^{WT} cells, we sequenced the transcriptomes

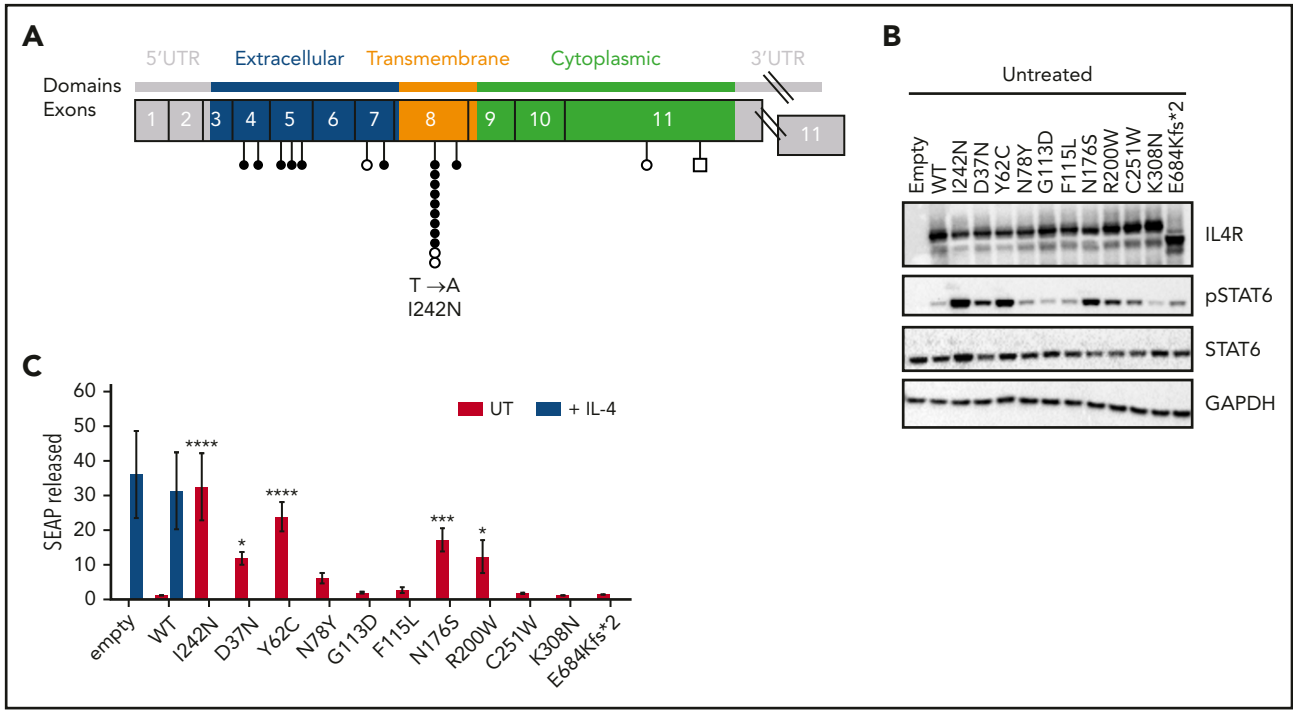

Figure 1. *IL4R* mutations in PMBCL and their ability to induce constitutive phosphorylation of STAT6 in HEK293 cells. (A) Distribution of IL4R mutations in PMBCL cell lines (n = 3) (○ and □), previously reported in Gunawardana et al[14] and PMBCL clinical samples (n = 62) (●) identified by targeted deep amplicon and Sanger sequencing. Missense and frameshift mutations are represented by circles and squares, respectively. Variations in noncoding regions, reported single nucleotide polymorphisms, and synonymous mutations are not shown. (B-C) HEK293-STAT6 cells were transfected with IL4R WT, IL4R mutants, or mock expression vector (empty) and either left UT or stimulated with human recombinant IL-4 (0.1 ng/mL) for 24 hours. (B) Western blot analysis of IL4R, pSTAT6, STAT6, and GAPDH in cell lysates. (C) STAT6-dependent SEAP released in cell-free supernatants. The values were normalized to untreated HEK293-STAT6 cells transfected with IL4R WT vector. (C) Mean ± SD of 3 independent experiments; significance was evaluated using 1-way ANOVA followed by Bonferroni post test. *$P < .05$; ***$P < .001$, ****$P < .0001$. SD, standard deviation; UT, untreated; UTR, untranslated region.

of both derivative cell lines by RNA-Seq. Forty-four genes were upregulated and 2 were downregulated in the mutant cell line compared with WT (fold change ≥0.6; Figure 3A; supplemental Tables 5 and 6). Of these, the B-cell activation marker CD23 (encoded by *FCER2*) and the thymus and activation-regulated chemokine (TARC; encoded by *CCL17*) were the most significantly upregulated genes in DEV IL4R^{I242N} cells (Figure 3A). In accord with the gene expression results obtained from the RNA-Seq analysis, we detected higher amounts of CCL17 by ELISA in the supernatant of DEV IL4R^{I242N} cells compared with DEV IL4R^{WT} (Figure 3B). Validation of CD23 upregulation was confirmed by flow cytometry (Figure 3C; supplemental Figure 7A) and real-time PCR (supplemental Figure 7B).

We next sought to examine if the upregulation of CD23 and CCL17 observed in DEV IL4R^{I242N} would also be reflected in primary PMBCL tumors. The Illumina Whole-Genome DASL assay revealed higher expression of both *CD23* and *CCL17* mRNA in lymphomas carrying the IL4R mutation compared with samples expressing WT IL4R (1.5 fold higher expression of *CD23* [$P < .05$] and *CCL17* [$P = .066$]) (supplemental Table 7).

We also investigated in primary cases if mutations in *IL4R* were capable of driving the PMBCL-specific gene expression profile previously described by Rosenwald and colleagues.[3] Indeed, cases carrying a mutation in *IL4R* were significantly associated (Q value < 0.001), with increased expression of the PMBCL gene signature, including *CCL17*, *PDCD1LG2*, and *CD23* (Figure 3D-E) in comparison with WT cases. Similarly, the PMBCL gene signature was enriched in cases carrying a mutation in *PTPN1* and *STAT6* (supplemental Figure 8A-D), but not in *SOCS1* (supplemental Figure 8E-F). Because *SOCS1* mutations are highly recurrent in PMBCL cases, we decided to distinguish the cases carrying either the *SOCS1* mutation alone vs the cases in which *SOCS1* mutations cooccurred with additional mutations in the JAK-STAT pathway (ie, *IL4R*, *PTPN1*, and *STAT6*). Only specimens having cooccurring mutations in *SOCS1* and *IL4R*, *PTPN1*, or *STAT6* showed significant correlation with the PMBCL-specific gene expression profile (supplemental Figure 8G-J).

Moreover, a significant overlap of differentially expressed genes ($P < .001$) was observed between DEV cells (IL4R^{I242N} vs IL4R^{WT}) and the primary PMBCL study cohort (n = 42; *IL4R* mutated vs *IL4R* WT) (supplemental Figure 9). Molecular pathway and biological processes analysis of both datasets using the DAVID tool showed enrichment of genes involved in inflammatory responses, immune responses, plasma membrane integrity, chemokine signaling, and cytokine receptor interactions (supplemental Table 8).

IL4R I242N mutation hyperphosphorylates STAT proteins but not JAKs

To delineate molecular mechanisms that might lead to constitutive activation of pSTAT5 and pSTAT6 in DEV IL4R^{I242N}, we investigated phosphorylation of JAK family members. Because of difficulties in the detection of JAK (JAK1, JAK2, JAK3, and TYK2) phosphorylation by conventional direct protein blotting,[25] we first immunoprecipitated tyrosine-phosphorylated protein and subsequently immunoblotted with antibodies that recognize JAK1, JAK2, JAK3,

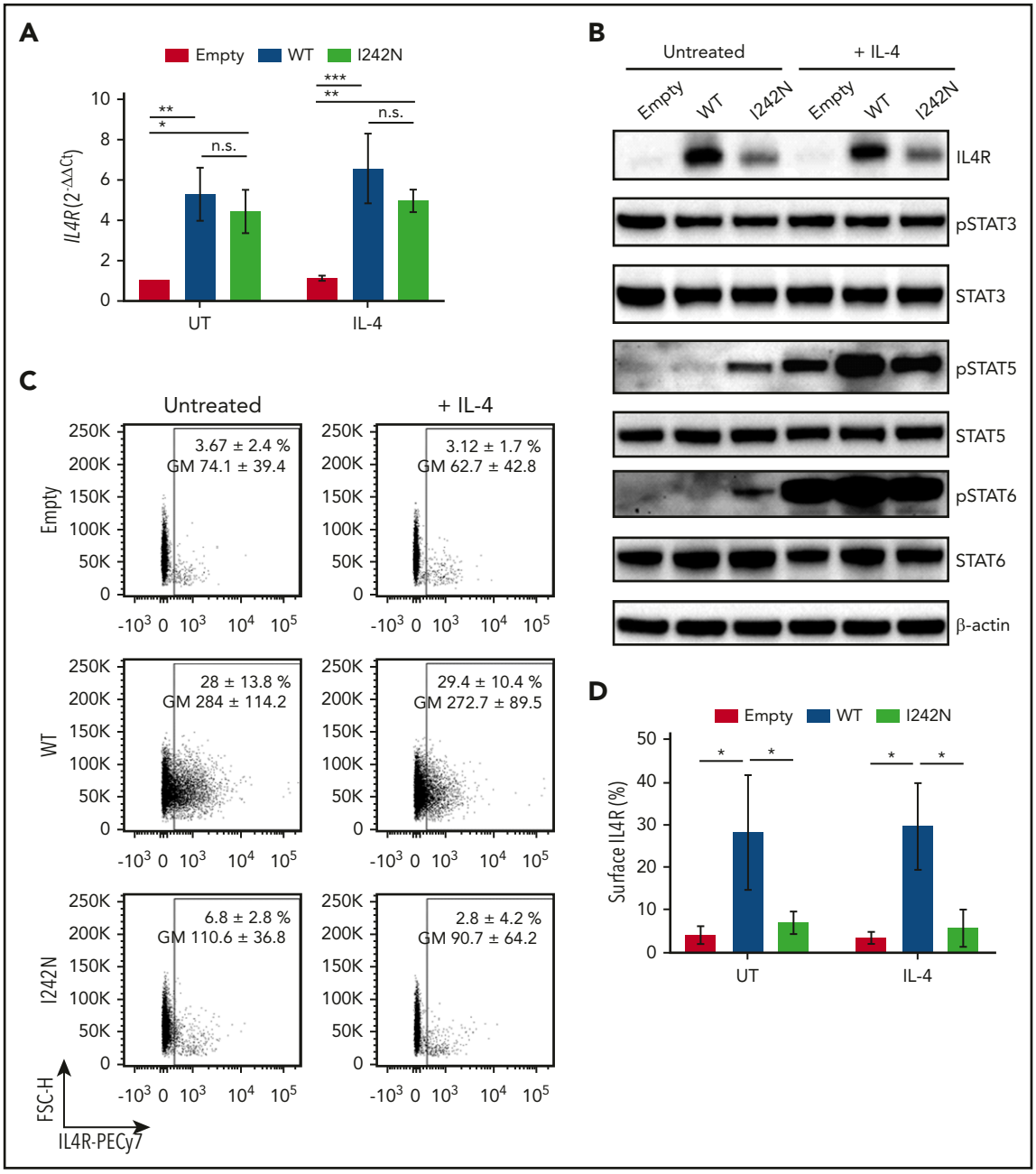

Figure 2. IL4R I242N mutant induced STAT activation in DEV cells. Transduced DEV cells with retrovirus control (empty) or retrovirus expressing IL4R WT or hotspot I242N mutant under control of doxycycline (20 ng/mL, 48 hours) were treated with human recombinant IL-4 (20 ng/mL) for (A,C-D) 24 hours, (B) 20 minutes, or left UT. (A) mRNA expression of *IL4R* measured by quantitative real-time PCR. (B) Phosphorylation status of STAT3, STAT5, and STAT6 and protein level of IL4R were determined by western blot. (C-D) Flow cytometry analysis of cell-surface expression of IL4R represented as a (C) scatter plot and (D) bar plot. (C) Numbers represent the mean ± SD of the percentage of IL4R-expressing cells and the respective GM; the scatter plots correspond to representative data of 3 independent experiments. (A,D) Graphs show the mean ± SD of 3 independent experiments; significance was evaluated using 1-way ANOVA with Tukey posttest. $*P < .05$; $**P < .01$; $***P < .001$. GM, geometric mean; n.s., nonsignificant.

and TYK2. Activation of all JAKs and TYK2 was observed in IL-4–treated DEV IL4R^{WT}, and their phosphorylation was decreased when cells were pretreated with a pan-JAK inhibitor (Pyridone 6) and a JAK2 inhibitor (Pacritinib) (Figure 4A). In comparison with DEV IL4R^{WT}, DEV IL4R^{I242N} showed a slightly lower phosphorylation of JAKs following the stimulation with the ligand that was not prevented by the inhibitors (Figure 4A). No activation of JAKs was observed in untreated DEV IL4R^{I242N} (Figure 4A), despite the constitutive activation of STATs. Because of the oncogenic role of the JAK-STAT pathway in PMBCL,[31] we explored the potential therapeutic effect of pacritinib on ameliorating STAT5 and STAT6 activation. Pacritinib treatment effectively inhibited IL-4–induced phosphorylation of STATs (supplemental Figure 10A-C), supporting the role of JAK2 during extrinsic receptor activation.[31,32] Conversely, pacritinib treatment only partially prevented the activation of STAT5 (Figure 4B; supplemental Figure 10C). Moreover, no inhibition of STAT6 constitutive phosphorylation (Figure 4B; supplemental Figure 10C) and no reduction of CD23 surface expression (Figure 4C; supplemental Figure 10D) were observed in pacritinib-treated IL4R^{I242N}.

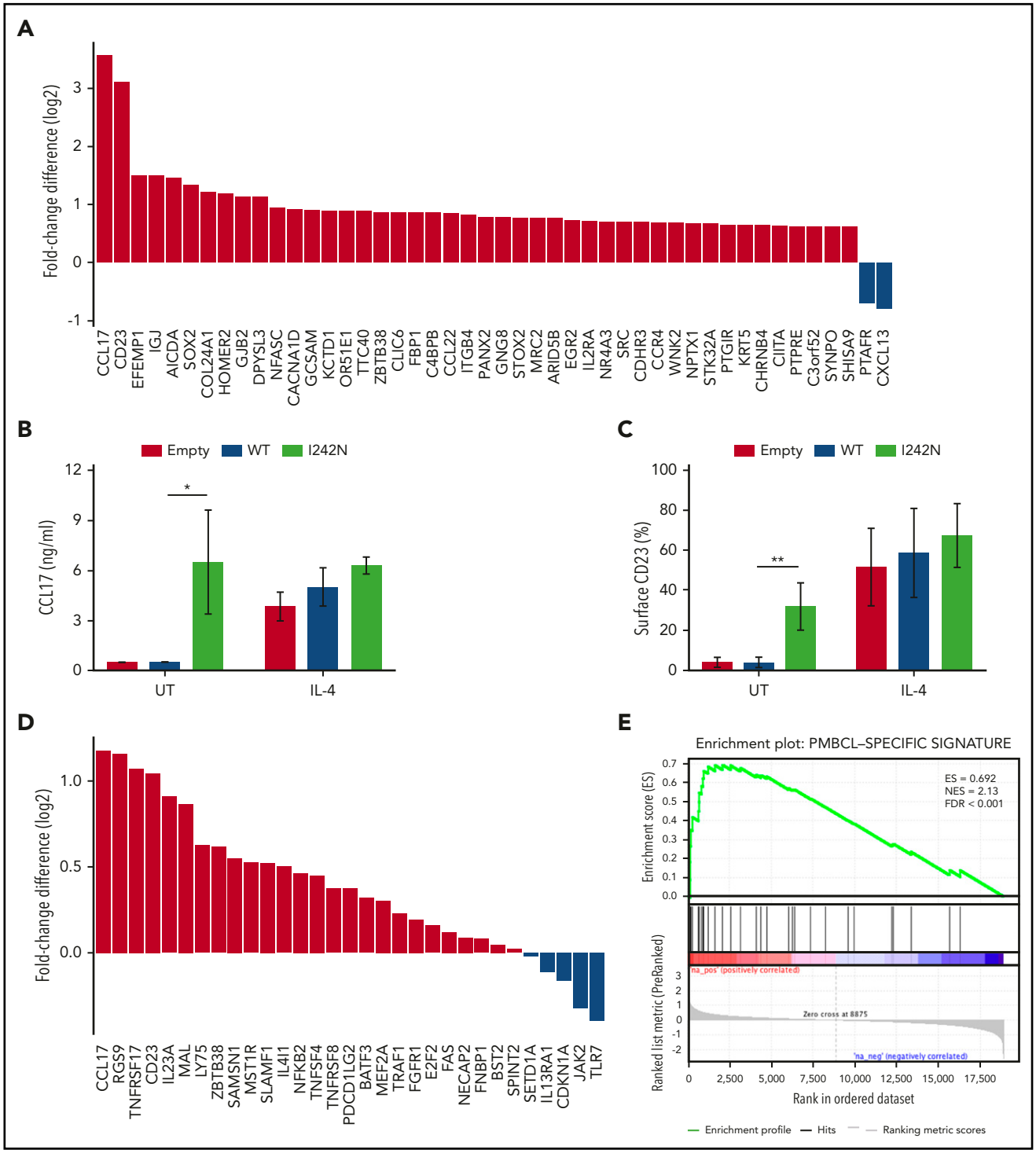

Figure 3. IL4R mutations led to CCL17 and CD23 expression as part of a PMBCL-characteristic phenotype. (A) Differential gene expression of RNA isolated from doxycycline-treated DEV IL4R^{WT} and IL4R^{I242N} cells by RNA-Seq. The most significantly changed genes are shown (Q value ≤ 0.01). (B-C) Transduced DEV cells with retrovirus control (empty) or retrovirus expressing IL4R WT or I242N mutant under control of doxycycline (20 ng/mL, 48 hours) were treated with human recombinant IL-4 (20 ng/mL) for 24 hours or left UT. (B) CCL17 released in supernatants by transduced DEV cells was measured by ELISA. (C) Flow cytometry analysis of cell-surface expression of CD23 represented as bar plot. (D-E) GSEA of the differential gene expression obtained from specimens overlapped with PMBCL gene-expression signature described in Rosenwald et al.[3] is represented as waterfall plot (D) and GSEA enrichment plot (E). (B-C) Graphs show the mean ± SD of 3 (B) or 4 (C) independent experiments and significance evaluated using 2-sample 2-tailed Student *t* test. *$P < .05$; **$P < .01$. ES, enrichment score; FDR, false discovery rate; GSEA, gene-set enrichment analysis; NES, normalized enrichment score.

IL4R I242N xenografts promote tumor formation and decrease survival in transplanted mice

We next evaluated the tumorigenic role of *IL4R* mutations in vivo. DEV cells transduced with *IL4R*^{I242N} and *IL4R*^{WT} were injected subcutaneously into the back of female NSG mice. In contrast to animals xenografted with *IL4R*^{WT} cells, mice xenografted with *IL4R*^{I242N} cells formed larger tumors by day 20 (mean, 211.7 mm^3 in mutant vs mean, 55.0 mm^3 in WT; $P < .01$; Figure 5A) and these

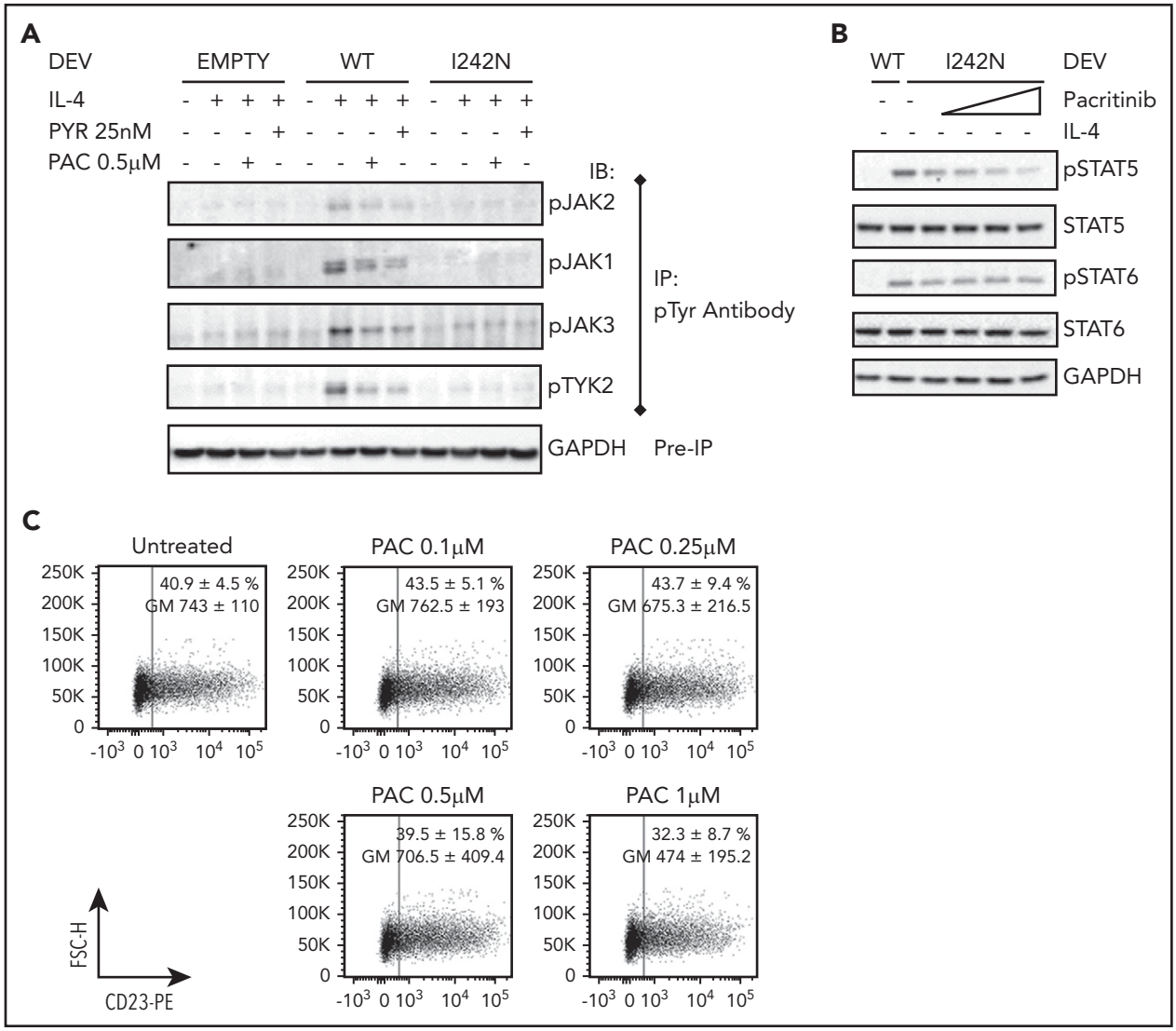

Figure 4. *IL4R*-I242N induced STAT6 but not JAK2 activation in DEV cells. Transduced DEV cells with retrovirus control (empty) or retrovirus expressing IL4R WT or I242N mutant under control of doxycycline (20 ng/mL, 48 hours) were pretreated with PYR or PAC for (A-B) 2 or (C) 24 hours followed by stimulation with (A) human recombinant IL-4 (20 ng/mL) for 20 minutes or (B,C) left UT. (A) Immunoblot analysis of JAKs (JAK1, JAK2, JAK3, and TYK2) phosphorylation was performed following IP with an anti-phosphotyrosine (*p*-Tyr) antibody. GAPDH analysis in samples before IP was used as a loading control. (B) Phosphorylation status of STAT5 and STAT6 were determined by western blot in DEV cells pretreated with PAC (0.1, 0.25, 0.5, and 1 μM). (C) Flow cytometry analysis of cell-surface expression of CD23 in DEV transduced with IL4R I242N mutant represented as a scatter plot. Numbers represent the mean ± SD of the percentage (%) and GM of CD23 expressing cells and the scatter plots correspond to a representative experiment. IP, immunoprecipitation; PAC, pacritinib; PYR, pyridone 6.

mice showed inferior overall survival (50% of mutant mice survived only 29 days compared with 50% of WT mice who survived 41 days; $P < .01$; Figure 5B). Consistent with our in vitro results, ex vivo tumors obtained from *IL4R*^{I242N} xenografted mice expressed significantly higher levels of *CCL17* and *FCER2* mRNA while showing similar *IL4R* expression (Figure 5C). To determine if differences in tumor volumes are attributed to increased cell proliferation of transplanted DEV IL4R^{I242N} cells, we investigated the proliferation rate of DEV IL4R^{WT} and DEV IL4R^{I242N} cells in xenograft tumors using H&E and Ki67 staining of tumor sections. We found significantly more Ki67^{+} cells in DEV IL4R^{I242N} compared with DEV IL4R^{WT} (Figure 5D-E), consistent with increased in vivo cell proliferation in tumors expressing mutant IL4R. Interestingly, no differences in proliferation between DEV IL4R^{WT} and DEV IL4R^{I242N} cells were detected in vitro (supplemental Figure 11).

The JAK-STAT pathway is frequently targeted in PMBCL

Complete mutational data for the JAK-STAT pathway genes *PTPN1, IL4R, SOCS1, STAT6*, and fluorescence in situ hybridization results for *JAK2* gain/amplification were available for 30 primary PMBCL cases (Figure 6A). In line with data published in the literature, we found frequent mutations in JAK-STAT pathway genes, and 27/30 (90%) of the cases harbored at least 1 genetic alteration in the genes/chromosomal areas analyzed and 19/30 (63.3%) of the cases had 2 or more genetic hits (Figure 6A). *SOCS1* was the most frequently mutated gene (53.33%), followed by *STAT6* (43.33%), *JAK2* gain/amplification (40.74%), *PTPN1* (26.66%), and *IL4R* (20%). We then assessed downstream targets of the JAK-STAT pathway (eg, pSTAT6, CD23, CCL17) by immunohistochemistry and observed that they significantly

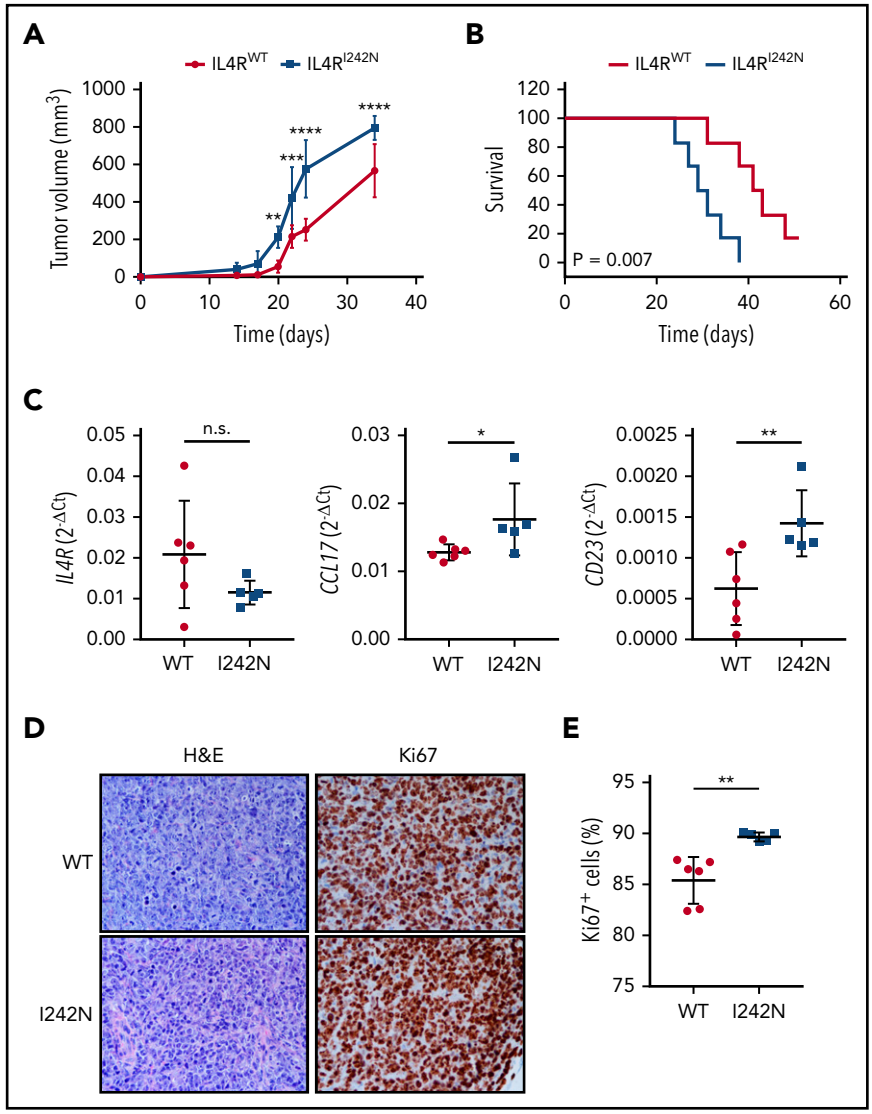

Figure 5. *IL4R*-I242N induced tumorigenesis in murine xenografts. (A) Tumor volume and (B) Kaplan-Meier survival curves from NSG mice xenografted with DEV cells expressing IL4R^{WT} (n = 6) or IL4R^{I242N} (n = 5). (C) mRNA expression of *IL4R*, *CCL17*, and *CD23* measured by quantitative real-time PCR in xenograft tumors. (D-E) Ki67 and H&E staining performed in xenograft tumors. (D) Representative IHC images are shown and the (E) percentage of Ki67$^+$ cells was measured using automatic cell counting with ImageJ. Images were acquired using Eclipse E600 microscope, DS-F1 camera, and DS-L2 acquisition software (Nikon); original magnification ×40; numerical aperture of objective lenses, 0.75. Graphs show the mean ± SD and significance evaluated using 2-way ANOVA with (A) Bonferroni posttest and (C,E) 2-sample unpaired 2-tailed Student *t* test. *$P < .05$; **$P < .01$; ***$P < .001$; ****$P < .0001$.

correlate with each other (Figure 6A-B). Specimens with 2 or more JAK-STAT pathway hits were significantly more often positive for at least 1 of those markers compared with cases with 1 or no genetic aberrations (Fisher exact test $P < .05$) (Figure 6A-B).

Discussion

In the present work, we confirmed the high prevalence of recurrent somatic aberrations affecting the JAK-STAT pathway in PMBCL. Using targeted sequencing, we described novel and recurrent *IL4R* missense mutations in PMBCL (24.2%) with a hotspot mutation in exon 8 affecting the transmembrane domain of the IL4R protein. This hotspot single nucleotide variant, encoding an I242N substitution, acts as a gain-of-function mutation leading to constitutive activation of the oncogenic JAK-STAT pathway that guides an altered cytokine profile.

Mutations in *IL4R* have been sporadically identified in solid tumors[33-37] and lymphoid cancers[14,38,39] but, up to now, no previous studies have elucidated the mechanism of *IL4R* mutations in B-cell lymphoma. Here, we identified novel mutations that are spread across all domains (extracellular, transmembrane, and cytoplasmic) of IL4R in PMBCL. Among all the mutations discovered, the I242N hotspot mutation represented >56% (9/16) of the primary cases, suggesting its ability to confer a tumorigenic advantage. The hotspot mutation (I242N) is located in the transmembrane domain, which is highly conserved between species and composed of numerous hydrophobic amino acids (ie, isoleucine, leucine, and valine), which can be involved in binding/recognition of hydrophobic ligands. Indeed, the conversion of transmembrane residues to potentially charged amino acids has been shown to alter the fate of transmembrane proteins, affecting their translocation to the surface and leading to endoplasmic reticulum retainment and degradation.[40] This could explain the reduction in the amount of global and surface IL4R protein observed in cells expressing the IL4R^{I242N}. Recently, Kurgonaite and colleagues described the importance of increased internal local concentration of IL4R to initiate the downstream JAK-STAT signaling transduction.[41] Therefore, the accumulation of mutant IL4R in the endoplasmic reticulum could allow the initiation of ligand-independent signaling. Previous reports showed the presence of heterozygous activating mutations in another type I cytokine receptor, IL7R, in T-cell acute lymphoblastic leukemia.[42,43] Similar to the hotspot mutation

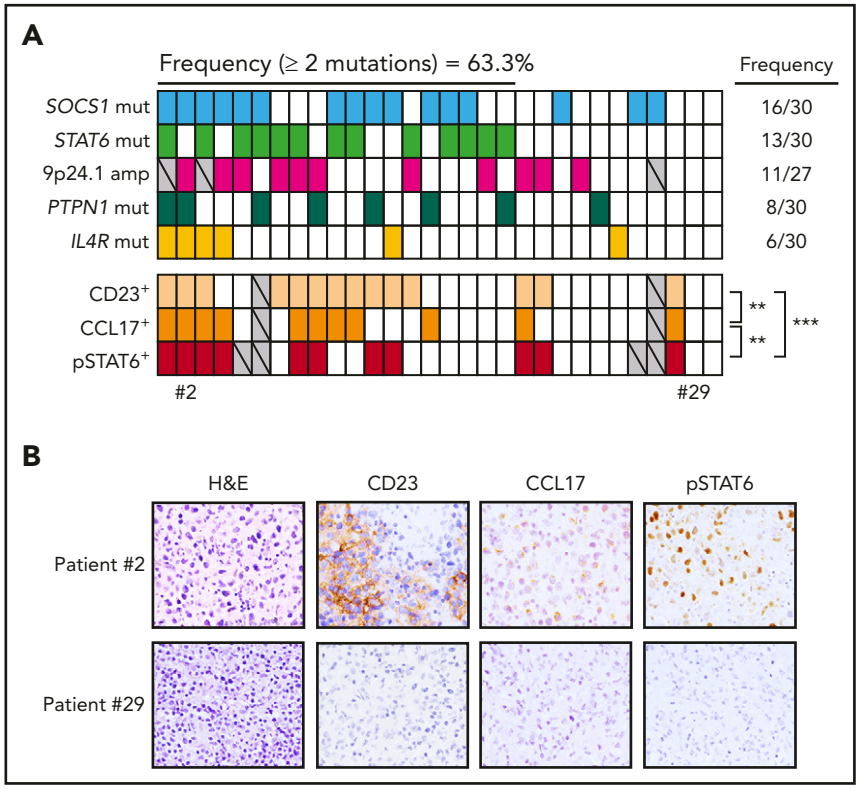

Figure 6. Aberrations in the JAK-STAT pathway in PMBCL. The frequency and presence of aberrations affecting 5 genes (*SOCS1, STAT6, JAK2, PTPN1, IL4R*) are displayed in the first 5 rows for 30 PMBCL patients. Each column represents a patient, and rows are ordered by the presence of mutations from the most to the least frequently mutated gene. For each patient, IHC analysis of CD23, CCL17, and pSTAT6 are displayed (staining is considered positive when the percentage of positive cells is ≥10%); significant correlation was evaluated using 2-sided Fisher exact test. $^{**}P < .01$; $^{***}P < .001$. Gray, data not evaluable. (B) Representative IHC sections stained with H&E, CD23, pSTAT6, and CCL17. Images were acquired using an Eclipse E600 microscope, DS-F1 camera, and DS-L2 acquisition software (Nikon); original magnification ×40; numerical aperture of objective lenses, 0.75.

observed here in IL4R, noncysteine in-frame mutations affecting the transmembrane domain of IL7R led to ligand-independent activation of the JAK-STAT signaling pathway and induced tumorigenesis in vivo.[43] However, mutations in IL7R did not affect global and surface protein levels. Also, in contrast to IL7R mutations, the IL4R hotspot mutation did not stabilize the receptor oligomerization in vitro (data not shown), suggesting the involvement of a different mechanism of activation. It has been reported that STAT activation can occur without the involvement of JAKs.[44-46] Interestingly, we did not observe constitutive activation of JAKs in cells expressing IL4R^{I242N}, suggesting that IL4R^{I242N} might induce STAT activation in a noncanonical fashion.

The JAK-STAT signaling pathway is tightly regulated under physiological conditions, and its aberrant activation is a hallmark of lymphoma pathogenesis. In agreement with published data in the field, genetic alterations in PMBCL affecting the JAK-STAT pathway (such as *JAK2, STAT6, SOCS1*, and *PTPN1*)[12,14,47] occurred in the majority of cases analyzed (90%). Our data show that 63.3% of the primary specimens analyzed harbor multiple mutational hits in the JAK-STAT pathway, suggesting additive/synergistic effect of mutations that contribute to the deregulation of this pathway and the pathogenesis of PMBCL. Immunohistochemistry data confirmed that the hyperactivation of the JAK-STAT pathway leads to an increase in pSTAT6, CD23, and CCL17 protein expression. CD23 and CCL17 are highly expressed in PMBCL and HL compared with DLBCL and have been used as part of a molecular signature proposed to discriminate PMBCL from DLBCL,[3] which also includes genes such as *MAL, NFKB2, LY75, PDCD1LG2, IL4I1*, and *TNFSF4*. Our data strongly suggest that mutations in the JAK-STAT pathway have an additive effect in contributing to PMBCL pathogenesis and regulating the expression of CD23 and CCL17. Our experimental in vitro studies in DEV cells explicitly demonstrate upregulated CD23 and CCL17 expression in cells harboring mutant IL4R. Signaling through CD23 has been reported to induce mitogen-activated protein kinase pathway activation through the phosphorylation of ERK1/2,[48,49] which can in turn regulate cell proliferation. This could explain the increased ERK1/2 phosphorylation observed in IL4R^{I242N} in vitro. Moreover, CD23 can be released as soluble fragments and have an autocrine/paracrine effect. Indeed, CD23 has been shown to sustain the growth of a human pre–B-acute lymphocytic leukemia cell line,[50] adding another possible explanation for the increased proliferation observed in IL4R^{I242N} in vivo.

In B-cell lymphoma, the survival of malignant lymphocytes is not only driven by cell-intrinsic mechanisms, but is also modulated by the interaction with cells and soluble molecules present in the microenvironment. The microenvironment of PMBCL resembles to some extent that of HL,[4] which has been extensively investigated.[17,51] CCL5, CCL17, and CCL22 chemokines are highly expressed by HL tumor cells[52] and secreted in the microenvironment, where they attract CCR4$^+$ tumor promoting cells, such as CD4$^+$ T cells and T regulatory cells.[53-55] No mutations in *IL4R* have been found in HL cases (data not shown and previous studies[56,57]). Here we establish a link between somatic *IL4R* mutations and CCL17 expression in B cells. Indeed gain-of-function mutation in IL4R led to a significant increase in expression and release of CCL17 in vitro and in vivo. We speculate that this might be one of the mechanisms by which tumor cells orchestrate a pro-tumorigenic microenvironment. In parallel to the T-cell recruitment mediated by CCL17, activation of the JAK-STAT signaling pathway in B cells can also induce the expression of the coregulatory molecules PDL1/PDL2,[58] which negatively regulate T-cell function, allowing PMBCL tumors to acquire an immune escape phenotype.

In summary, we have discovered novel recurrent somatic mutations in the cytokine receptor *IL4R* and demonstrate that the hotspot mutation in exon 8 constitutively activates the JAK-STAT signaling pathway. Our data suggest that these activating mutations contribute to the remodeling of the microenvironment and pathogenesis of PMBCL, with implications for future treatment strategies.

Acknowledgments

The authors thank the British Columbia Cancer Foundation and the Canada Foundation for Innovation for their support. We also thank the Genome Sciences Centre production group and the Centre for Applied Genomics for excellent technical support.

This work is supported by a research grant by the Canadian Institute of Health Research (#2202) and Terry Fox Research Institute team grants (#1023 and #1061) (C.S.). J.G. was supported by the Roman M. Babicki fellowship in Medical Research. A.M. was supported by fellowship awards from the Mildred Scheel Cancer foundation (Deutsche Krebshilfe), the Michael Smith Foundation for Health Research (MSFHR), and Lymphoma Canada. R.K. was supported by fellowship awards by CIHR, MSFHR, and UBC.

Authorship

Contribution: E.V. and J.G. designed and performed the research, analyzed and interpreted data, and wrote the manuscript; A.M. performed research, analyzed and interpreted immunohistochemistry data, and revised the manuscript; T.V.T., K.M., E.C., B.W., K.T., D.T., A.T., O.K., S.H., S.B.-N., R.K., and A.D. performed experiments and interpreted data; F.C.C., L.C., H.P.S., and S.S.H. analyzed amplicon sequencing, RNAseq, and complementary DNA-mediated annealing, selection, extension, ligation data; K.J.S., L.R., K.L., P.G., R.G. provided study material; C.S. designed the research, interpreted data, and wrote the manuscript; and all authors reviewed the manuscript.

Conflict-of-interest disclosure: The authors declare no competing financial interests.

Correspondence: Christian Steidl, Department of Lymphoid Cancer Research, British Columbia Cancer Agency, 675 West 10th Ave, Vancouver, BC V5Z 1L3, Canada; e-mail: csteidl@bccancer.bc.ca.

Footnotes

Submitted 29 September 2017; accepted 8 February 2018. Prepublished online as *Blood* First Edition paper, 21 February 2018; DOI 10.1182/blood-2017-09-808907.

*E.V. and J.G. contributed equally to this work.

The data reported in this article have been deposited in the European Genome-phenome Archive (accession number EGAS00001002796).

Presented partially in abstract form at the 106th annual meeting of the American Association for Cancer Research, Philadelphia, PA, 18-22 April 2015.

The online version of this article contains a data supplement.

The publication costs of this article were defrayed in part by page charge payment. Therefore, and solely to indicate this fact, this article is hereby marked "advertisement" in accordance with 18 USC section 1734.

REFERENCES

1. Savage KJ. Rare B-cell lymphomas: primary mediastinal, intravascular, and primary effusion lymphoma. *Cancer Treat Res*. 2008;142:243-264.

2. Alizadeh AA, Eisen MB, Davis RE, et al. Distinct types of diffuse large B-cell lymphoma identified by gene expression profiling. *Nature*. 2000;403(6769):503-511.

3. Rosenwald A, Wright G, Leroy K, et al. Molecular diagnosis of primary mediastinal B cell lymphoma identifies a clinically favorable subgroup of diffuse large B cell lymphoma related to Hodgkin lymphoma. *J Exp Med*. 2003;198(6):851-862.

4. Savage KJ, Monti S, Kutok JL, et al. The molecular signature of mediastinal large B-cell lymphoma differs from that of other diffuse large B-cell lymphomas and shares features with classical Hodgkin lymphoma. *Blood*. 2003;102(12):3871-3879.

5. Campo E, Swerdlow SH, Harris NL, Pileri S, Stein H, Jaffe ES. The 2008 WHO classification of lymphoid neoplasms and beyond: evolving concepts and practical applications. *Blood*. 2011;117(19):5019-5032.

6. Guiter C, Dusanter-Fourt I, Copie-Bergman C, et al. Constitutive STAT6 activation in primary mediastinal large B-cell lymphoma. *Blood* 2004;104(2):543-549.

7. Steidl C, Gascoyne RD. The molecular pathogenesis of primary mediastinal large B-cell lymphoma. *Blood*. 2011;118(10):2659-2669.

8. Bonizzi G, Karin M. The two NF-kappaB activation pathways and their role in innate and adaptive immunity. *Trends Immunol*. 2004;25(6):280-288.

9. Weniger MA, Gesk S, Ehrlich S, et al. Gains of REL in primary mediastinal B-cell lymphoma coincide with nuclear accumulation of REL protein. *Genes Chromosomes Cancer*. 2007;46(4):406-415.

10. Gu M, Wessendorf M. Endomorphin-2-immunoreactive fibers selectively appose serotonergic neuronal somata in the rostral ventral medial medulla. *J Comp Neurol*. 2007;502(5):701-713.

11. Schmitz R, Hansmann ML, Bohle V, et al. TNFAIP3 (A20) is a tumor suppressor gene in Hodgkin lymphoma and primary mediastinal B cell lymphoma. *J Exp Med*. 2009;206(5):981-989.

12. Green MR, Monti S, Rodig SJ, et al. Integrative analysis reveals selective 9p24.1 amplification, increased PD-1 ligand expression, and further induction via JAK2 in nodular sclerosing Hodgkin lymphoma and primary mediastinal large B-cell lymphoma. *Blood*. 2010;116(17):3268-3277.

13. Melzner I, Bucur AJ, Brüderlein S, et al. Biallelic mutation of SOCS-1 impairs JAK2 degradation and sustains phospho-JAK2 action in the MedB-1 mediastinal lymphoma line. *Blood*. 2005;105(6):2535-2542.

14. Gunawardana J, Chan FC, Telenius A, et al. Recurrent somatic mutations of PTPN1 in primary mediastinal B cell lymphoma and Hodgkin lymphoma. *Nat Genet*. 2014;46(4):329-335.

15. Twa DD, Chan FC, Ben-Neriah S, et al. Genomic rearrangements involving programmed death ligands are recurrent in primary mediastinal large B-cell lymphoma. *Blood*. 2014;123(13):2062-2065.

16. Shi M, Roemer MG, Chapuy B, et al. Expression of programmed cell death 1 ligand 2 (PD-L2) is a distinguishing feature of primary mediastinal (thymic) large B-cell lymphoma and associated with PDCD1LG2 copy gain. *Am J Surg Pathol*. 2014;38(12):1715-1723.

17. Scott DW, Gascoyne RD. The tumour microenvironment in B cell lymphomas. *Nat Rev Cancer*. 2014;14(8):517-534.

18. Vardhana S, Younes A. The immune microenvironment in Hodgkin lymphoma: T cells, B cells, and immune checkpoints. *Haematologica*. 2016;101(7):794-802.

19. Fowler NH, Cheah CY, Gascoyne RD, et al. Role of the tumor microenvironment in mature B-cell lymphoid malignancies. *Haematologica*. 2016;101(5):531-540.

20. Mottok A, Steidl C. Genomic alterations underlying immune privilege in malignant lymphomas. *Curr Opin Hematol*. 2015;22(4):343-354.

21. Mottok A, Woolcock B, Chan FC, et al. Genomic alterations in CIITA are frequent in primary mediastinal large B cell lymphoma and are associated with diminished MHC class II expression. *Cell Reports*. 2015;13(7):1418-1431.

22. Chong LC, Twa DD, Mottok A, et al. Comprehensive characterization of programmed death ligand structural rearrangements in B-cell non-Hodgkin lymphomas. *Blood*. 2016;128(9):1206-1213.

23. Rui L, Emre NC, Kruhlak MJ, et al. Cooperative epigenetic modulation by cancer amplicon genes. *Cancer Cell*. 2010;18(6):590-605.

24. Steidl C, Shah SP, Woolcock BW, et al. MHC class II transactivator CIITA is a recurrent gene fusion partner in lymphoid cancers. *Nature*. 2011;471(7338):377-381.

25. Rui L, Drennan AC, Ceribelli M, et al. Epigenetic gene regulation by Janus kinase 1 in diffuse large B-cell lymphoma. *Proc Natl Acad Sci USA*. 2016;113(46):E7260-E7267.

26. Morin RD, Mendez-Lago M, Mungall AJ, et al. Frequent mutation of histone-modifying genes in non-Hodgkin lymphoma. *Nature*. 2011;476(7360):298-303.

27. Pastore A, Jurinovic V, Kridel R, et al. Integration of gene mutations in risk prognostication for patients receiving first-line immunochemotherapy for follicular lymphoma: a retrospective analysis of a prospective clinical trial and validation in a population-based registry. *Lancet Oncol*. 2015;16(9):1111-1122.

28. Chatila TA. Interleukin-4 receptor signaling pathways in asthma pathogenesis. *Trends Mol Med*. 2004;10(10):493-499.

29. Jung T, Schrader N, Hellwig M, Enssle KH, Neumann C. Soluble human interleukin-4 receptor is produced by activated T cells under the control of metalloproteinases. *Int Arch Allergy Immunol*. 1999;119(1):23-30.

30. Jung T, Wagner K, Neumann C, Heusser CH. Enhancement of human IL-4 activity by soluble IL-4 receptors in vitro. *Eur J Immunol*. 1999; 29(3):864-871.

31. Meier C, et al. Recurrent numerical aberrations of JAK2 and deregulation of the JAK2-STAT cascade in lymphomas. *Mod Pathol*. 2009; 22(3):476-487.

32. Aboudola S, Murugesan G, Szpurka H, et al. Bone marrow phospho-STAT5 expression in non-CML chronic myeloproliferative disorders correlates with JAK2 V617F mutation and provides evidence of in vivo JAK2 activation. *Am J Surg Pathol*. 2007;31(2):233-239.

33. Guo G, Sun X, Chen C, et al. Whole-genome and whole-exome sequencing of bladder cancer identifies frequent alterations in genes involved in sister chromatid cohesion and segregation. *Nat Genet*. 2013;45(12): 1459-1463.

34. Krauthammer M, Kong Y, Ha BH, et al. Exome sequencing identifies recurrent somatic RAC1 mutations in melanoma. *Nat Genet*. 2012; 44(9):1006-1014.

35. Peifer M, Fernández-Cuesta L, Sos ML, et al. Integrative genome analyses identify key somatic driver mutations of small-cell lung cancer. *Nat Genet*. 2012;44(10):1104-1110.

36. Frattini V, Trifonov V, Chan JM, et al. The integrated landscape of driver genomic alterations in glioblastoma. *Nat Genet*. 2013; 45(10):1141-1149.

37. Kan Z Zheng H, Liu X, et al. Whole-genome sequencing identifies recurrent mutations in hepatocellular carcinoma. *Genome Res*. 2013; 23(9):1422-1433.

38. Pasqualucci L, Khiabanian H, Fangazio M, et al. Genetics of follicular lymphoma transformation. *Cell Reports*. 2014;6(1):130-140.

39. Mareschal S, Dubois S, Viailly PJ, et al. Whole exome sequencing of relapsed/refractory patients expands the repertoire of somatic mutations in diffuse large B-cell lymphoma. *Genes Chromosomes Cancer*. 2016;55(3): 251-267.

40. Bonifacino JS, Cosson P, Shah N, Klausner RD. Role of potentially charged transmembrane residues in targeting proteins for retention and degradation within the endoplasmic reticulum. *EMBO J*. 1991;10(10):2783-2793.

41. Kurgonaite K, Gandhi H, Kurth T, et al. Essential role of endocytosis for interleukin-4-receptor-mediated JAK/STAT signalling. *J Cell Sci*. 2015;128(20):3781-3795.

42. Zenatti PP, Ribeiro D, Li W, et al. Oncogenic IL7R gain-of-function mutations in childhood T-cell acute lymphoblastic leukemia. *Nat Genet*. 2011;43(10):932-939.

43. Shochat C, Tal N, Gryshkova V, et al. Novel activating mutations lacking cysteine in type I cytokine receptors in acute lymphoblastic leukemia. *Blood*. 2014;124(1):106-110.

44. Chen H, Sun H, You F, et al. Activation of STAT6 by STING is critical for antiviral innate immunity. *Cell*. 2011;147(2):436-446.

45. Gao X, Wang H, Yang JJ, Liu X, Liu ZR. Pyruvate kinase M2 regulates gene transcription by acting as a protein kinase. *Mol Cell*. 2012;45(5):598-609.

46. Sawka-Verhelle D, Tartare-Deckert S, Decaux JF, Girard J, Van Obberghen E. Stat 5B, activated by insulin in a Jak-independent fashion, plays a role in glucokinase gene transcription. *Endocrinology*. 2000;141(6): 1977-1988.

47. Mottok A, Renné C, Seifert M, et al. Inactivating SOCS1 mutations are caused by aberrant somatic hypermutation and restricted to a subset of B-cell lymphoma entities. *Blood*. 2009;114(20):4503-4506.

48. Chan MA, Gigliotti NM, Matangkasombut P, Gauld SB, Cambier JC, Rosenwasser LJ. CD23-mediated cell signaling in human B cells differs from signaling in cells of the monocytic lineage. *Clin Immunol*. 2010; 137(3):330-336.

49. Griffith QK, Liang Y, Onguru DO, Mwinzi PN, Ganley-Leal LM. CD23-bound IgE augments and dominates recall responses through human naive B cells. *J Immunol*. 2011;186(2): 1060-1067.

50. White LJ, Ozanne BW, Graber P, Aubry JP, Bonnefoy JY, Cushley W. Inhibition of apoptosis in a human pre-B-cell line by CD23 is mediated via a novel receptor. *Blood*. 1997; 90(1):234-243.

51. Herreros B, Sanchez-Aguilera A, Piris MA. Lymphoma microenvironment: culprit or innocent? *Leukemia*. 2008;22(1):49-58.

52. Maggio EM, Van Den Berg A, Visser L, et al. Common and differential chemokine expression patterns in rs cells of NLP, EBV positive and negative classical Hodgkin lymphomas. *Int J Cancer*. 2002;99(5):665-672.

53. Imai T, Baba M, Nishimura M, Kakizaki M, Takagi S, Yoshie O. The T cell-directed CC chemokine TARC is a highly specific biological ligand for CC chemokine receptor 4. *J Biol Chem*. 1997;272(23):15036-15042.

54. Imai T, Nagira M, Takagi S, et al. Selective recruitment of CCR4-bearing Th2 cells toward antigen-presenting cells by the CC chemokines thymus and activation-regulated chemokine and macrophage-derived chemokine. *Int Immunol*. 1999;11(1):81-88.

55. Iellem A, Mariani M, Lang R, et al. Unique chemotactic response profile and specific expression of chemokine receptors CCR4 and CCR8 by CD4(+)CD25(+) regulatory T cells. *J Exp Med*. 2001;194(6):847-853.

56. Reichel J, Chadburn A, Rubinstein PG, et al. Flow sorting and exome sequencing reveal the oncogenome of primary Hodgkin and Reed-Sternberg cells. *Blood*. 2015;125(7): 1061-1072.

57. Tiacci E, Döring C, Brune V, et al. Analyzing primary Hodgkin and Reed-Sternberg cells to capture the molecular and cellular pathogenesis of classical Hodgkin lymphoma. *Blood*. 2012;120(23):4609-4620.

58. Gravelle P, Burroni B, Péricart S, et al. Mechanisms of PD-1/PD-L1 expression and prognostic relevance in non-Hodgkin lymphoma: a summary of immunohistochemical studies. *Oncotarget*. 2017;8(27): 44960-44975.